

DOI: 10.24425/118949

B. GÜLSEREN*, O. BYCHKOV**, I. FROLOV***, M. SCHAPER*, O. GRYPIN**

SINKING OF ULTRA-THICK-WALLED DOUBLE-LAYERED ALUMINIUM TUBES

This work deals with the tube sinking process. The main purpose is to develop a process chain for the manufacturing of ultra-thick-walled tubes with the lowest possible diameter. The base material is a hot extruded tube consisting the aluminium alloy AA6063 with the dimensions $9,9 \times 1$ mm. The drawing tools include several dies with various exit holes, a drawing bench and a muffle oven to produce ultra-thick-walled tubes with dimensions $5,02 \dots 5,03 \times 1,54 \dots 1,59$ mm. The process has been applied successfully. With a double-layered tube, it was possible to reach a low diameter/wall-thickness ratio of 3,3 at tube sinking process. Subsequent pull-out tests showed that by reaching the threshold outer tube diameter value of $\varnothing 5$ mm the joining strength increased from 1,3 MPa to 6,2 MPa. It could be observed that the heat treatment reduced the joining strength for the double-layered tubes with diameter of 5 mm, whereupon for the bigger tubes diameter it has no significant influence on the joining strength.

Keywords: Tube sinking, double-layered tube, tube pull-out test, aluminium alloy AA6063

1. Introduction

The tube drawing process can be divided in four categories (see Fig. 1). One technique uses a fixed plug inside the tube, which leads to a better inner surface and a relatively homogenous wall-thickness. Similar to that process is the tube drawing with a floating plug, which is not fixed to a long rod. Another possibility is the use of a moving mandrel. While drawing, the tube and the mandrel are pulled simultaneously. The tube sinking process is conducted without any help of internal tools [1].

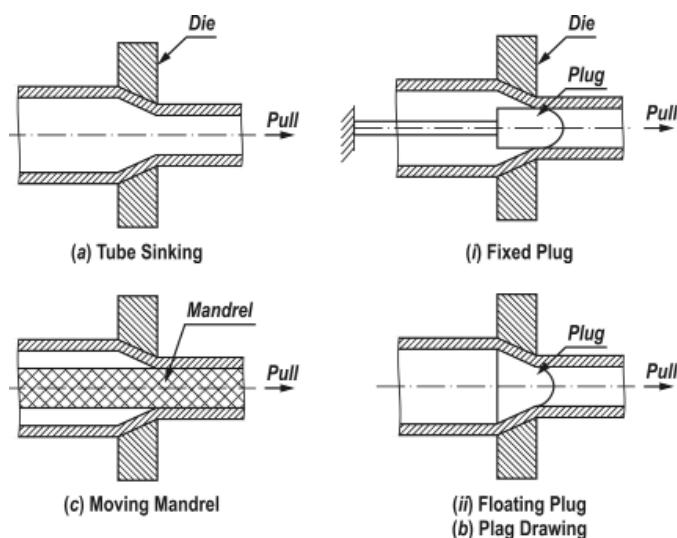


Fig. 1. Types of tube drawing [2]

All types of tube drawing are based on the fact, that the tube end must be first pushed through the conical opening of the drawing die and then get tightened by a puller which is attached to the carriage of the drawing machine [3]. The application of lubricants is necessary to reduce friction, tool wear and temperature. Otherwise the tube may break during the drawing process [4]. The drawn tubes have a closer dimensional accuracy, increased surface finish and improved mechanical properties due to strain-stress state at this process as well as strain hardening [5,6]. The effect of hardening was proven by Sawamiphakdi et al. with the help of hardness measurements before and after drawing [7]. The tube drawing offers the possibility to produce tubes with specific characteristics and irregular shapes, which cannot be realized by conventional hot forming processes like hot extrusion. The main process variables are [2]: mechanical properties of workpiece, speed of drawing, die angle, temperature, coefficient of friction, application of lubricant, cross-section reduction.

Fig. 2 shows schematically the tube sinking process. A tube with an original outer radius R_o and inner radius R_i is pulled through a conical die of a semi-cone angle α , having an exit hole of radius R_{of} . The initial wall-thickness s_o is characterized by $R_o - R_i$. The radius of the tube shrinks to R_{of} after passing through the drawing die. It may happen that the out coming diameter of the tube is a bit smaller than the exit of the die [8]. The wall-thickness slightly increases in the inside direction. Hence, the inner surface becomes progressively rougher, which can lead to cracking. The increase can be described as a function of friction and initial wall-thickness/diameter ratio [9].

* PADERBORN UNIVERSITY, CHAIR OF MATERIALS SCIENCE, WARBURGER STR. 100, 33100 PADERBORN, GERMANY

** NATIONAL METALLURGICAL ACADEMY OF UKRAINE, CHAIR OF METAL FORMING, GAGARINA AVE. 4, 49600 DNIPROPETROVSK, UKRAINE

Corresponding author: grydin@lwk.upb.de

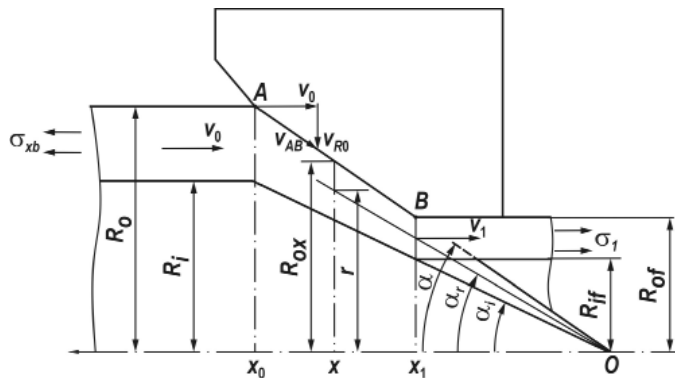


Fig. 2. Deformation zone in tube sinking [10]

A typical die angle is 12° and the bearing length is relatively long for the dimensional accuracy such as roundness. A lower angle is used to increase the wall-thickness, a higher angle to reduce it [11]. The optimal die angle reduces the drawing stress. Too low angles increase the contact length of tube and die. Too large angles minimize the friction, but cause distortion and redundant-power losses [10]. Bui et al. [12] discovered that the cross-section reduction during the tube sinking process has a significant influence on the mechanical properties of aluminium tubes. The investigation showed that after a cross-section reduction of 36% leads to a three times higher yield strength compared to the initial tube. The maximum possible cross-section reduction can be described as a function of friction coefficient and die angle [10]. In the paper [13] it was shown, that the level of diameter reduction has a significant influence on changes of metal properties.

For obtaining ultra-thick-walled tubes with a low diameter, the tube sinking is required. By using this method, there is no limitation according to the inner diameter of drawn tubes. Moreover, the tube sinking is the least costly of all drawing methods [14].

The idea of a cheap future production of ultra-thick-walled tubes can be derived from the functional principle of multiple die wire machine. After each drawing step the cross-sectional area of the wire is reduced, whereas length and speed are increased proportionally. Hence, the peripheral speed of each coil must be increased as well to avoid slippage. Two possible options are the use of several motors with adjustable speed or the use of stepped cones, as shown above [14].

The final product of the tube sinking process depends on the process parameter, tools and dimensions of the base-tube. The idea of this work is to develop a process chain for the sinking of ultra-thick-walled double-layered tubes. It proposed to deal as follows: put a previously drawn to semi-finished diameter tube inside a base tube and to restart the sinking process of the double-layered tube. Such tube at the end of the production gives the possibility to receive a lower D_o/s_o ratio, which results in a growth of wall-thickness.

The ultra-thick-walled aluminium tubes can be applied instead of stainless steel pipes in liquid and gas transportation and distribution systems with elevated pressure at a temperature

range from -45°C to $+60^\circ\text{C}$. Main advantages of such tubes are low price and weight as well as good workability and high heat capacity and conductivity of aluminium. In addition, using of double-layered tubes enables lower bending radii in comparison with monometallic products due to a possibility of the relative layers sliding.

2. Materials and methods

Overall 10 hot extruded base-tubes with the dimensions of $9,9 \times 1$ mm and a total length of 1,5 m were used. The material consists of the aluminium alloy AA6063-O (soft-annealed) which chemical composition is shown in Tab. 1. Due to its maximum possible elongation of 30%, it has a high formability [15]. The ultimate yield strength and shearing strength are 90 MPa and 70 MPa, respectively [16].

TABLE 1

Chemical composition of AA6063-O

Element	Si	Fe	Cu	Mn	Mg	Cr	Zn
Mass-%	0,47	0,17	0,01	0,03	0,45	0,003	0,004

The tube sinking experiments were performed using a chain drawing bench. The belonging characteristics are illustrated in Tab. 2.

TABLE 2

Characteristics of chain drawing bench

Chain drawing bench	
Engine power	4,5 kW
Engine rotational speed	1.440 turnover/min
Velocity of drawing process	0,188 m/s
Max. drawing force	23,9 kN
Assortment of drawing circle D	3-13 mm
Max. length of drawing	4100 mm

The drawing dies were put in the die holder. The outer diameter at the end of each tube was reduced sufficiently by cold swaging to enter the hole of the first used drawing die ($\varnothing 9,5$ mm). The swaging was repeated after several sinking steps, if necessary. Then the end was held tightly by the gripper of the carriage. Next, the tube was pulling through the die at a constant speed of 0,188 m/s. Before each sinking step, a standard oil based lubricant was applied.

Fig. 3 presents the sequence of the first conducted series of experiment, starting from an initial tube diameter of 9,9 mm and is followed by multiple sinking processes with a final die diameter of 5,0 mm without any intermediate heat treatment. Therefore, it was required to draw a tube progressively until the outer diameter reached 7 mm. The drawn tube was placed inside the bigger initial tube. The double-layered tube was drawn through the sequence 9,5 mm \rightarrow 5 mm.

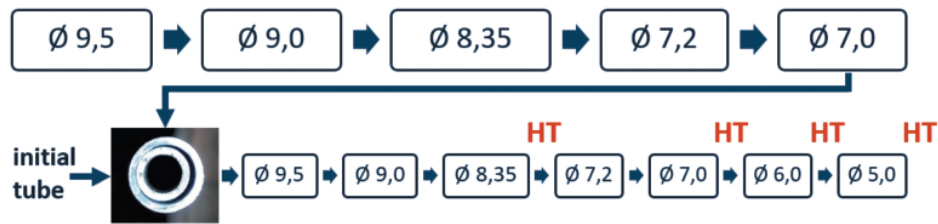


Fig. 3. Double-layered tube sinking schedule

Analogously, in the second series of experiments the double-layered tube sinking was repeated by using intermediate heat treatments (marked as HT in the Fig. 3) between the deformation steps.

For experiments a set of drawing dies, provided by an aluminium tubes manufacturer was used. The set was conventionally used in technological process chain for the tube drawing. Reduction angle of the applied dies varied in the range from 11° to 15° in accordance to practical recommendations [1,11]. The length of bearing surface was 3,5 mm for dies of diameters between 9,5 mm and 7,0 mm as well as 3 mm for dies \varnothing 6 and \varnothing 5 mm.

Cold forming processes lead to internal residual stresses in the workpiece [17]. Hence, the experiments were repeated by conducting intermediate stress relief heat treatments between two sinking steps. The heat treatment took place below the recrystallization temperature of AA6063 to reduce residual stresses without changing the structure. Therefore, a muffle oven with a thermocouple was used. In the first step, the oven was heated up until the environment reached a temperature of $350\text{--}370^\circ\text{C}$. Then the tubes were placed inside for about 3-5 minutes, followed by a continuously cool-down in the oven until 250°C and an air-cooling. That kind of heat treatment process is recommended for the used material with the given dimensions by Melnikov and Bunova [18]. Furthermore, Bourget et al. investigated the bendability of cold-drawn 6063 aluminium tubes. It could be observed, that the bending performance is strongly influenced by the heat treatment [19].

After each sinking step there were cut samples for subsequent measurements and analysis. The digital light microscope Keyence VHX-5000 was used to measure the geometric dimensions of tube cross-section. The specimens were cut to a length of 25 mm and embedded. After hardening of embedding, the observed cross-section surface was grinded and polished. Furthermore, the surface of the embedded tubes was etched to make the boundary between both layers clear visible.

The pull-out tests of 25 mm samples were conducted with the machine *MTS Landmark* to measure the joining strength between the outer and inner layers. The grip speed was adjusted to 8 mm/min. The test sequence was displacement-controlled. The scheme of the pull-out test is depicted in Fig. 4. Basically, the inner tube was pulled out of the outer tube. Therefore, two ordinary drill three-jaw chucks (pos. 1 and 4 in Fig. 4) had to be used. Two cylindrical adapters (pos. 7) were screwed in the backside of drill chucks and tightened by the chuck jaws (pos. 5) of the tensile test machine. One drill chuck gripped the outer tube

through a cylindrical aluminium nut (pos. 6). To grip the inner layer, an internal screw thread was tapped, following by inserting a steel screw (pos. 2), which was held by the second drill chuck.

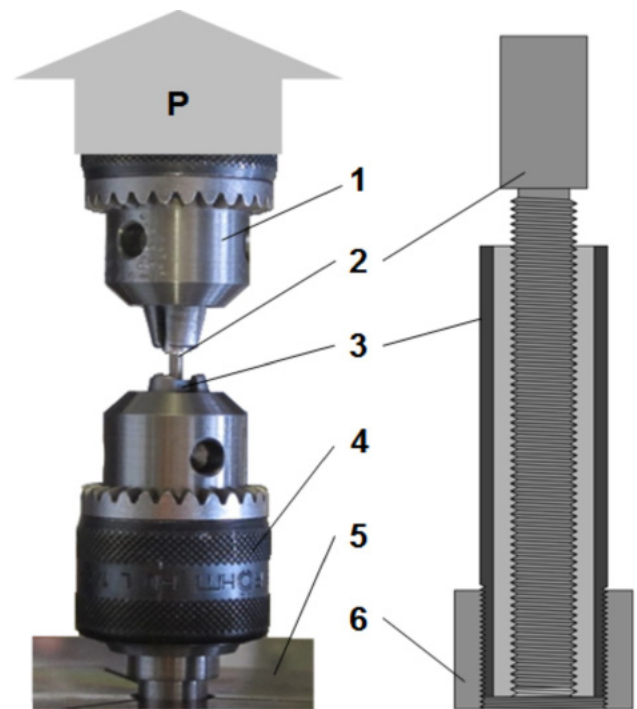


Fig. 4. Scheme of the pull-out test of the double-layered aluminium tubes: 1 – upper chuck; 2 – steel screw; 3 – double-layered tube; 4 – lower chuck; 5 – chuck jaw of the tensile test machine; 6 – cylindrical aluminium nut; 7 – cylindrical adapter

The biggest challenge at these tests was to fix the inner layer on the one end and the outer layer on the other side without an affecting of the joining strength of the interface. The triangular shape of the jaws is disadvantageous for gripping the outer layer. It would deform the specimen and wouldn't ensure a sufficient friction between jaws and tube surface. Hence, the inside of the chucks has to be grinded first, so that the three jaws will build a round hole while tightening. Then an internal screw thread was trapped to increase the friction. In addition, the tube diameter was measured before and after the pull-out test. For the tubes (with heat treatment) with an outer diameter of 5 mm and an inner diameter of ca. 2 mm, a two-component zinc-dust epoxy of the type *3M DP490* and a spring steel wire had to be used. The adhesive hardening took place at 65°C for 2 hours. It was important not to tighten the tubes too much, otherwise it would deform which can influence the measurement results.

3. Results and discussion

Fig. 5 shows the micro sections of two-layer specimens (with heat treatment)– after passing a die with an exit hole of \varnothing 8,35 mm, resp. \varnothing 5,0 mm.

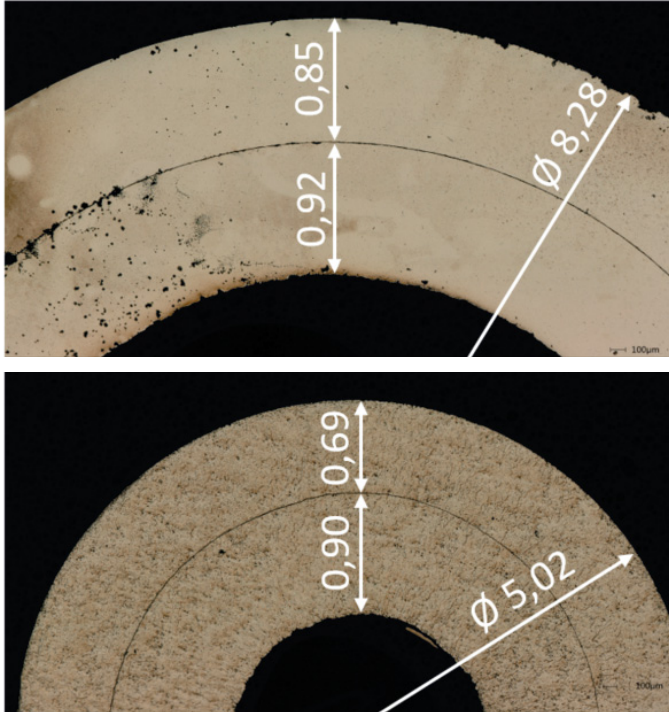


Fig. 5. Micro sections of two-layered specimens with heat treatment, above: after sinking step 3, with an outer diameter of 8,28 mm, below: after sinking step 7, with an outer diameter of 5,02 mm

The dimensions of all two-layered specimens are summarized in the Tab. 3.

TABLE 3

Geometric dimensions in mm of two-layered specimens, upper table: without heat treatment, lower table: with subsequent heat treatment (HT), “—” – not measured

<i>NoSinking</i>	1	2	3	4	5	6	7
<i>D_{die}</i>	9,5	9,0	8,35	7,2	7,0	6,0	5,0
<i>D_{outer}</i>	—	—	8,38	7,2	—	5,98	5,03
<i>D_{inner}</i>	—	—	4,92	3,83	—	2,75	1,95
<i>s_{outer}</i>	—	—	0,84	0,78	—	0,70	0,62
<i>s_{inner}</i>	—	—	0,88	0,90	—	0,91	0,92
<i>s_{sum}</i>	—	—	1,73	1,68	—	1,61	1,54
<i>D_{outer}</i>	—	—	8,27	7,15	—	5,89	5,02
<i>D_{inner}</i>	—	—	4,73	3,63	—	2,61	1,85
<i>s_{outer}</i>	—	—	0,85	0,84	—	0,77	0,69
<i>s_{inner}</i>	—	—	0,92	0,92	—	0,87	0,90
<i>s_{sum}</i>	—	—	1,77	1,76	—	1,64	1,59

Fig. 6 shows the course of the diameter of inner and outer layer after sequence of sinking the steps. It can be seen that the heat treatment between sinking steps has no significant effect on the change of the measured diameters.

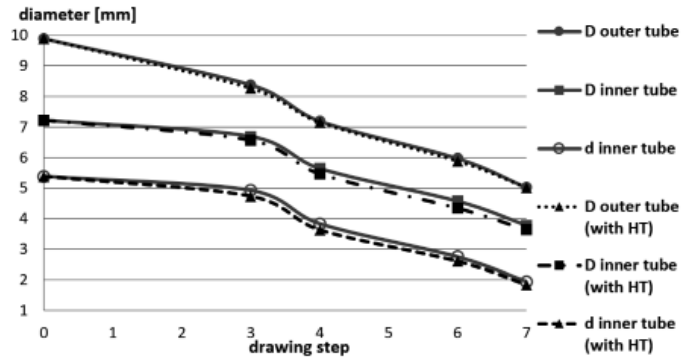


Fig. 6. Change of diameter after sequence of sinking steps

The change of the wall-thickness after each sinking step is shown in Fig. 7.

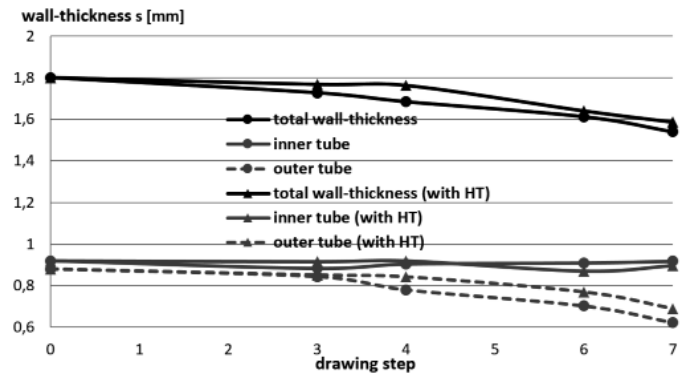


Fig. 7. Change of wall-thickness after sequence of sinking steps

There is a slight decrease of the wall-thickness of the outer tube for heat treated and not heat treated tubes, whereas the inner tube remains constant. The maximal difference between thicknesses of outer (0,62 mm) and inner (0,92 mm) layers could be seen after last sinking step at not heat treated tube. In general, the total wall-thickness decreases.

Fig. 8 illustrates the elastic deformation related to the diameter after sequence of sinking steps. The outer diameters of the drawn tubes don't correspond to the exit diameter of the dies (see Tab. 3). Usually the tube diameter expanded after sinking due to the effect of elastic deformation.

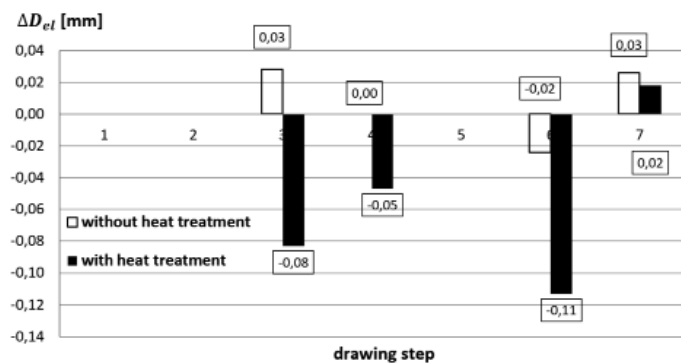


Fig. 8. Elastic diameter-related deformation after sequence of sinking steps

A negative change of outer tube diameter is a consequence of the plastic deformation. The drawing force was higher than the yield strength of the material, which has been reduced by annealing. A higher yield strength corresponds to a higher resilience of the material. There is no identifiable trend indicating a homogenous diameter deformation. Looking at the values of the tubes with heat treatment, the diameter-strain decreased at sinking steps 3, 4 and 6 after corresponding annealing.

Fig. 9 shows the forming zone of a double-layered tube (without heat treatment) with an initial diameter of 8,35 mm passing a die with an exit hole of \varnothing 7,2 mm.

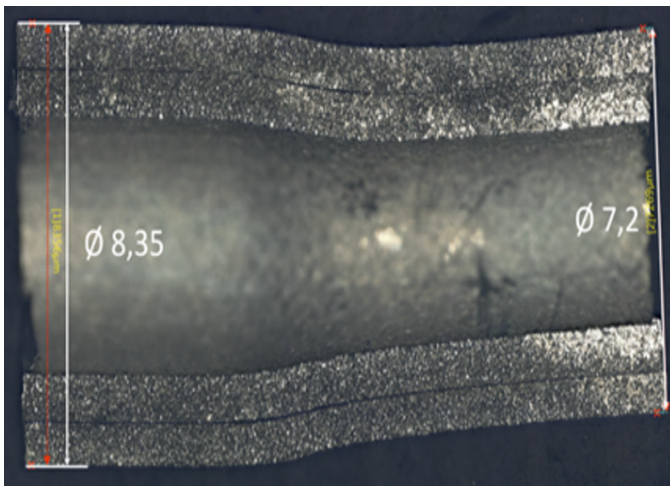


Fig. 9. Forming zone of double-layered tube with \varnothing 8,35 mm while passing die hole \varnothing 7,2 mm

The transition from the initial to the out coming diameter and the material boundaries are clearly visible. The maximum gap between the two layers is located in the main forming zone. The right half of the tube seems to be a little bit curved. Its axis is tilted at a certain angle. It illustrates the well-known problem of the drawing, related with inhomogeneous friction around the tube perimeter. The information can serve as basis for further simulations.

Above mentioned experimental procedure of tube pull-out test is appropriated only for qualitative comparison of the level of joining strength between the tube layers. All experiments were carried out with approximately equal clamping force, as well as the clamped length. To recalculate "Pull-out stress against displacement" diagram from the data, obtained from the test machine. The loading force was divided by the continuously decreased area of the contact surface ($A = 2\pi r\Delta l$, whereas $\Delta l = \text{joining length} - \text{axial displacement}$). The example of the tube pull-out tests results is given in form of a pull-out stress/displacement graph (Fig. 10).

The graphs show an absence of significant influence of HT for \varnothing 6 mm. On the first millimeter of displacement for both samples the pull-out stress falls, after a relatively intensive growth to a maximal value of 1,1...1,3 MPa, with the same intensity to values less than 0,1 MPa. The diagram can be characterized into three categories (A, B and C). On the ascent of the curve,

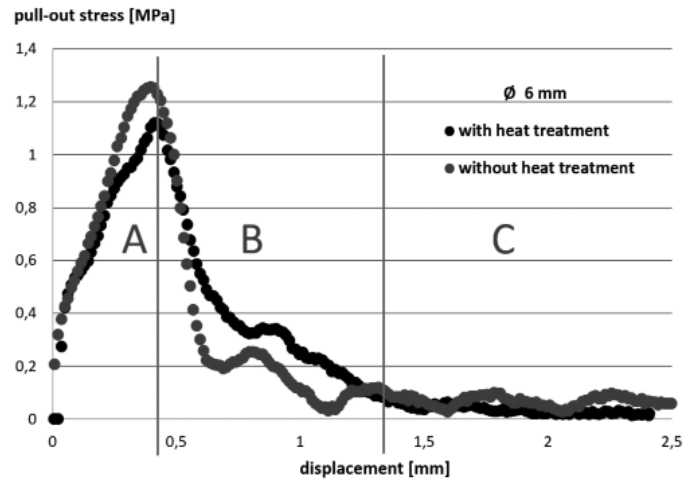


Fig. 10. Pull-out stress against displacement (example of single specimens; \varnothing 6 mm)

the main mechanism for joining is based on form-fit (section A). The touching surfaces of the layers have a certain roughness given by the base material and some more irregularities caused by decreasing of perimeter of both tubes during the sinking process. By reaching the maximum joining strength, the layers begin to slide relatively to each other (section B). Lower stress values at the end of measurement reflect dynamic friction of rejected contact surfaces (section C). The results of the samples with \varnothing 6 mm are characteristic for tubes with bigger diameters, which show a similar joining strength.

Fig. 11 gives an example of a typical pull-out stress/displacement graph for sample with \varnothing 5 mm, which shows a maximal joining strength of 6,2 MPa. In contrast to the tests for the \varnothing 6 mm double-layered tubes, it was reached in two stages of curve development. The first stage, analogous to the \varnothing 6 mm tubes, looks like the elastic part of a tensile diagram. For the second stage, the plastic behavior of sample is characteristic, which is similar to stress-strain curves at tensile or shear tests. Such plastic flow stage of the curve could be described both as a shear deformation localized in the near-interface areas of tubes or as a tensile deformation of the inner layer. Analogous to stress-strain diagrams from tensile tests values for the yield stress and strength in the elastic range can be characterized. According to the diagram (Fig. 11) the plastification of the material starts at 3,51 MPa. Similar to the previous diagram, the characteristic sections A, B and C can be shown. The stress of metal's plastification begin at the pull-out test for the heat treated \varnothing 5 mm double-layered tubes amounted to 1,73 MPa, whereas the maximum joining strength for the specimens after heat treatment reached 2,2 MPa. However, it is to mention, that the initial roughness of the tubes surfaces was not considered before conducting of sinking and pull-out tests. The results show that probably the roughness of contact surfaces as well as compress stresses on the interface between tube's layers, affected by reduction of diameters at finishing sinking steps, have a high influence on the curves course and the joining strength as well.

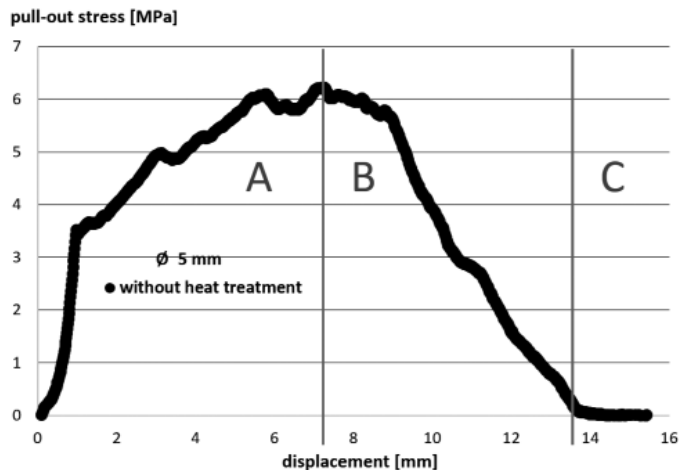


Fig. 11. Pull-out stress against displacement (example of single specimens; \varnothing 5 mm)

4. Conclusions and outlook

The experimental study shows that the suggested tube sinking process was appropriated for the manufacturing of an ultra-thick walled double-layered aluminium tube with a diameter/wall-thickness ratio of 3,3. Such low value of the ratio is not achievable with the one-layered tube sinking.

The microscopic pictures have shown, that the conducted inline heat treatment had no significant influence on the geometric dimensions for the material AA6063. The highest elastic diameter-related deformation was noticed by the sinking through the die of \varnothing 7,2 mm. Overall, the results for the elastic deformation are inhomogeneous. The influence of each deformation parameters such as die angle, friction coefficient and diameter reduction on the tube's elastic deformation requires further study. The total wall-thickness of the two layers decreased continuously to 1,6 mm, which is still 70% more than the wall-thickness of a one-layered tube, using the same tool parameters. Until the sixth sinking step (\varnothing 6 mm) the change of the outer diameter did not lead to an increase of the joining strength. By reaching the threshold tube diameter value (\varnothing 5 mm) the joining strength increased sharply. It could be observed that the heat treatment reduced the joining strength for the double-layered tubes with diameter of 5 mm, whereupon for the bigger tubes diameter it has no significant influence on the joining strength.

The influence of initial tubes roughness on joining strength requires further scientific studies. Furthermore, the complex method for examining the pull-out stress between the tube layers has to be optimized.

Acknowledgement

The authors would like to thank the German Academic Exchange Service (DAAD) for the financial support within the scope of the project "Praxispartnerschaft Metallurgie".

REFERENCES

- [1] V.N. Danchenko, Metal forming: text-book – NMetAU, 183, 2007, Dnepropetrovsk.
- [2] P.C. Sharma, Production Technology: Manufacturing Processes, 2007, S. Chand Publishing New Delhi, G.E. Dieter, H.A. Kuhn, S.L. Semiatin, Handbook of Workability and Process Design, 2003 ASM International, Ohio.
- [3] L. Shaheen, Tube drawing principles; Understanding processes, parameters key to quality, TPJ - The Tube & Pipe J., 2007, T.Z. Blazynski, Plasticity and Modern Metal-Forming Technology, 1989 Elsevier, New York.
- [4] G.E. Dieter, H.A. Kuhn, S.L. Semiatin, Handbook of Workability and Process Design, 2003 ASM International, Ohio, P.C. Sharma, Production Technology: Manufacturing Processes, 2007 S. Chand Publishing, New Delhi.
- [5] P. Karnezis, D.C.J. Farrugia, Study of cold tube drawing by finite-element modelling, J. of Mater. Proc. Techn. **80-81**, 690-694 (1998), DOI:10.1016/S0924-0136(98)00127-7.
- [6] T.Z. Blazynski, Plasticity and Modern Metal-Forming Technology, 1989 Elsevier, New York.
- [7] K. Sawamiphakdi, G.D. Lahoti, P.K. Kropp, Simulation of a tube drawing process by the finite element method, J. of Mater. Proc. Techn. **27**(1-3), 179-190 (1991), DOI:10.1016/0924-0136(91)90052-G.
- [8] B. Avitzur, Handbook of metal forming processes, 2. [Dr.], 1983 Wiley, New York.
- [9] O. Pawelski, U. Ruediger, Berechnung der Wanddickenänderung beim Hohlzug von Rohren, Arch. Eisenhüttenwes. **47**, 483-487 (1976).
- [10] D.W. Zhao et al., An analytical solution for tube sinking by strain rate vector inner-product integration, J. of Mater. Proc. Techn., 408-415 (2009), DOI:10.1016/j.jmatprotec.2008.02.011.
- [11] B. Boljanovic, Metal Shaping Processes Casting and Molding Particulate Processing Deformation Processes and Metal Removal, 2009 Industrial Press Inc., New York.
- [12] Q.H. Bui, X.T. Pham, M. Fafard, Modelling of microstructure effects on the mechanical behavior of aluminium tubes drawn with different reduction areas, Int. J. of Plast. **50**, 127-145 (2013), DOI:10.1016/j.ijplas.2013.04.005.
- [13] J.R. Davis, Aluminum and aluminum alloys, 1994 Metals Park, Ohio.
- [14] G.E. Totten, Handbook of Residual Stress and Deformation of Steel, 2002 ASM International, Ohio.
- [15] A.A. Melnikov, G.Z. Bunova, Heat treatment technology of aluminium wrought product, textbook for coursework, State University of Aerospace Engineering, 2005, Samara.
- [16] J.P. Bourget et al., Optimization of heat treatment in cold-drawn 6063 aluminium tubes, J. of Mater. Proc. Techn. **209**(11), 503-504 (2009), DOI:10.1016/j.jmatprotec.2009.01.027.